

Is there a single surge mechanism? Contrasts in dynamics between glacier surges in Svalbard and other regions

Tavi Murray

School of Geography, University of Leeds, Leeds, UK

Tazio Strozzi¹ and Adrian Luckman

Department of Geography, University of Wales, Swansea, UK

Hester Jiskoot² and Panos Christakos

School of Geography, University of Leeds, Leeds, UK

Received 31 March 2002; revised 24 October 2002; accepted 30 December 2002; published 9 May 2003.

[1] During the 1990s, Monacobreen, a 40-km-long tidewater glacier in Svalbard, underwent a major surge. We mapped the surge dynamics using ERS synthetic aperture radar images, differential dual-azimuth interferometry and intensity correlation tracking. A series of 11 three-dimensional (3-D) velocity maps covering the period 1991–1997 show a months-long initiation and years-long termination to the surge, with no indication of a surge front travelling downglacier. During the surge, the front of the glacier advanced ~ 2 km, the velocity and derived strain rate increased by more than an order of magnitude, and maximum ice flow rates measured during 1994 were ~ 5 m d⁻¹. The spatial pattern of both velocity and strain rate was remarkably consistent and must therefore be controlled by spatially fixed processes operating at the glacier bed. We combine these results with those published in the literature to construct a typical Svalbard glacier surge cycle and compare this to surge dynamics of glaciers from other cluster regions, especially those of Variegated Glacier in Alaska. The strong contrast in dynamics suggests that there exist at least two distinct surge mechanisms. *INDEX TERMS*: 1863 Hydrology: Snow and ice (1827); 0933 Exploration Geophysics: Remote sensing; 9315 Information Related to Geographic Region: Arctic region; 1827 Hydrology: Glaciology (1863); *KEYWORDS*: glacier surging, glacier dynamics, interferometry, Svalbard, synthetic aperture radar (SAR), remote sensing

Citation: Murray, T., T. Strozzi, A. Luckman, H. Jiskoot, and P. Christakos, Is there a single surge mechanism? Contrasts in dynamics between glacier surges in Svalbard and other regions, *J. Geophys. Res.*, 108(B5), 2237, doi:10.1029/2002JB001906, 2003.

1. Introduction

[2] A surge-type glacier experiences cyclic flow that alternates between decades of slow flow and shorter periods of flow that is typically 10–1000 times faster. Less than 1% of Earth's glaciers are believed to surge [Jiskoot *et al.*, 2000], but surge-type glaciers are of great importance in the understanding of glacier dynamics. The two-phase flow regime shows that profound changes occur in processes and conditions beneath the glacier that allow it to switch between fast and slow flow despite only small changes in driving stress.

[3] In order to comprehend the mechanisms of glacier surging it is important to search for systematic differences in surge dynamics between regions. Many surge-type glaciers are situated in remote locations, and a surge may be

completely missed or be well under way before it is recognized. Archives of remotely sensed data provide a valuable resource for studying glacier dynamics and allow long-term studies that would logistically be difficult in situ. Both surface topography and surface displacement can be measured using differential satellite radar interferometry (SRI) [Kwok and Fahnestock, 1996]. Dual-azimuth imagery from ascending and descending passes of the satellite in conjunction with a digital elevation model (DEM) can be used to resolve the 3-D ice velocity field [Mohr *et al.*, 1998; Joughin *et al.*, 1998]. However, because glacier surging is often associated with extreme ice velocities, SAR interferometry can be unsuitable for mapping ice dynamics. For example, Fatland and Lingle [1998] used interferometry to study the effects of the Bering Glacier surge on the Bagley icefield reservoir zone, but interferometric coherence was lost on the glacier itself because the ice was moving and deforming so rapidly. Similarly, studies on Storstrømmen in northeast Greenland [Mohr *et al.*, 1998] and Sortebrae, east Greenland [Murray *et al.*, 2002], were able to use interferometry only in the quiescent phase. However, the relatively low ice velocities and long duration that characterize surges

¹Also at Gamma Remote Sensing, Muri, Switzerland.

²Now at Department of Geography, University of Lethbridge, Calgary, Alberta, Canada.

in Svalbard [Dowdeswell *et al.*, 1991; Murray *et al.*, 1998] makes them amenable to study using interferometry [Dowdeswell *et al.*, 1999; Luckman *et al.*, 2002].

[4] In this paper, we use dual-azimuth differential radar interferometry to derive the flow dynamics of Monacobreen, a surge-type glacier in northern Svalbard, through seven years of its active phase. A preliminary analysis of the interferometric data has been presented by Luckman *et al.* [2002]. In this paper we also present the results of using intensity correlation tracking [Strozzi *et al.*, 2002] to determine the ice dynamics in regions of the glacier where flow rates exceed that measurable using interferometry, together with a glaciological interpretation of the data. The combination of these techniques allows us to determine glacier surface dynamics during the surge in unprecedented spatial and temporal detail which, together with published results, allows us to construct a typical Svalbard surge cycle. We compare this cycle to surge dynamics of glaciers from other cluster regions, especially those of Variegated Glacier in Alaska. The strong contrast in surge dynamics leads us to suggest that there exist at least two distinct surge mechanisms.

2. Location and Characteristics of Monacobreen

[5] Monacobreen (79°24'N, 12°34'E) is a 40-km-long, tidewater glacier (Figure 1) that descends northward from an elevation of ~1250 m on the Isachsenfonna ice cap and terminates in Liefdefjord. During the past century most glaciers in Svalbard have been in retreat from their maximal extent during the Little Ice Age, and aerial photographs acquired by Norsk Polarinstittutt (NP) show that the margin of Monacobreen retreated between 0.75 and 1.45 km between 1966 and 1990 (NP photographs S66V-4286 and S90 6568). The onset of heavy crevassing first noticed in May 1992 (J. O. Hagen, personal communication, 2001), together with marginal advance noted by comparing 1993 Landsat imagery with 1990 aerial photography, suggests that Monacobreen had begun to surge between 1990 and 1992.

[6] Radio echo sounding (RES) can be used to infer glacier thermal regime. RES suggests that Monacobreen is polythermal because an internal reflecting horizon (IRH) at a depth of ~120 to 200 m obscured any bed return, suggesting that the glacier has a warm-based upper region [Bamber, 1987].

[7] Monacobreen overlies two geological formations, which are separated by a fault running approximately NNW-SSE [Hjelle and Lauritzen, 1982]. The eastern part of the glacier, including the entire width of the front, is underlain by coarse conglomerates and sandstones. The western parts are underlain by a combination of granitic bands, gneisses, and schists. All of these geologic formations show various degrees of metamorphism and tectonism. Monacobreen terminates in a fjord and its terminus is probably underlain in part by Quaternary marine deposits.

3. Methods

3.1. Differential Interferometry

[8] We applied the usual procedure for differential interferometry [e.g., Joughin *et al.*, 1996a, 1996b] using either triplets from the 3-day repeat phases, or two pairs from the

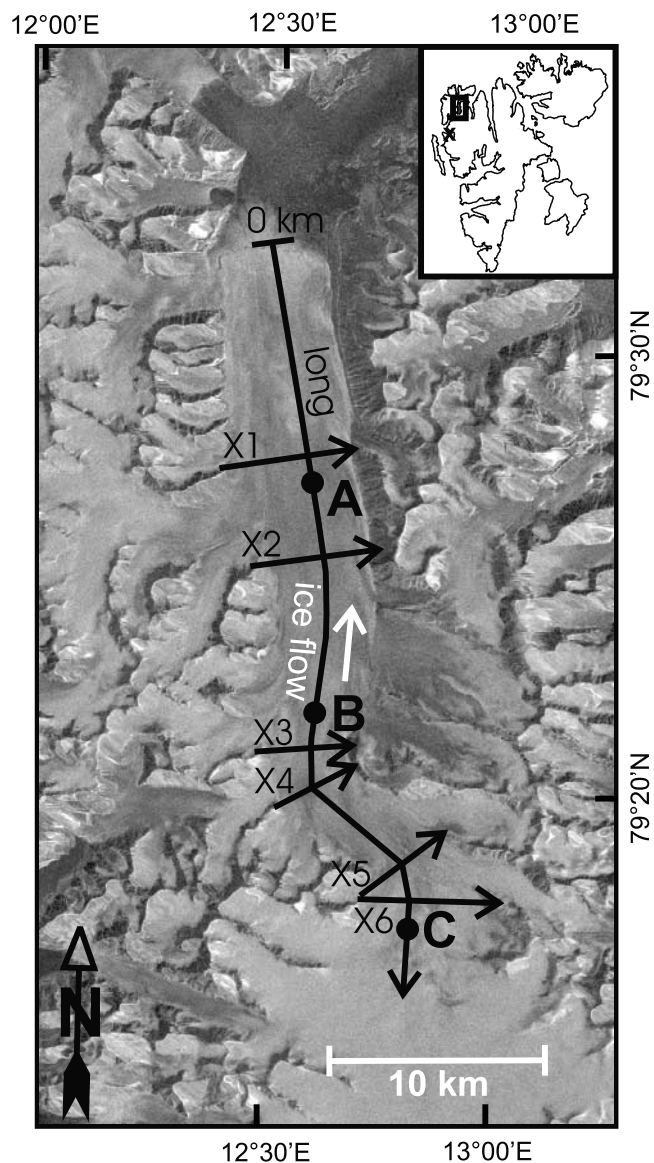


Figure 1. Location of Monacobreen (box in insert) and of meteorological station at Ny Ålesund (cross) in northern Spitsbergen. The locations of the long profile and cross profiles (X1–X6) are also shown. Profiles were extracted in the direction of arrows. The long profile is taken along an approximate flow line from 0 km at the 1995 margin to a point on the plateau and has a total length of 33.5 km. A, B, and C are the locations of points used in Figure 9 and are at km 10.3, km 20.0, and km 30.6, respectively. Background backscatter intensity image is from 28/29 December 1995. An IRH was seen on a radio echo sounding [Bamber, 1987] upglacier of X1, suggesting that this portion of the glacier was warm based.

tandem phase of ERS operation. In order to maximize phase coherence between pairs of ERS SAR images, we avoided periods with melting or precipitation and periods of strong winds following recent snow (Table 1). To help phase unwrapping of the differential topography only interferograms, we used a digital elevation model (DEM) derived from mapping by NP (digital versions of 1:100,000 map

Table 1. Dates and Characteristics of Images and Interferometric Combinations Used to Determine the Flow Evolution of the Surge

Image Dates	Orbit	Frame	Perpendicular Baseline, m	Topography Baseline, ^a m	Date of Resulting Velocity Map
<i>Descending Pass Images</i>					
4–7 Sept. 1991	E-708/E1-751	1989 ^b	–184	↓	Sept. 1991
13–16 Oct. 1991	E1-1267/E1-1310	1989 ^b	–82	160	Oct. 1991
16–19 Oct. 1991	E1-1310/E1-1353	1989 ^b	–242		
15–18 Nov. 1991	E1-1740/E1-1783	1989 ^b	163	↑	Nov. 1991
10–13 Feb. 1992	E1-2987/E1-3030	1989	87	↓	Feb. 1992
23–26 March 1992	E1-3589/E1-3632	1989	74	137	March 1992
26–29 March 1992	E1-3632/E1-3675	1989	–63		
12–15 Jan. 1994	E1-13037/E1-13080	1971 ^b	177	93	Jan. 1994
15–18 Jan. 1994	E1-13080/E1-13123	1971 ^b	84		
28–31 March 1994	E1-14112/E1-14155	1974 ^b	141	↑	March 1994
1–2 June 1995	E1-20280/E2-607	1981	–2	↓	June 1995
28–29 Dec. 1995	E1-23286/E2-316	1981	–38	–206	Dec. 1995
1–2 Feb. 1996	E1-23787/E2-4114	1981	168		
30 April to 1 May 1996	E1-25061/E2-5388	1980 ^b	–35	–41	May 1996 ^c
3–4 May 1996	E1-25104/E2-5431	1976 ^b	6		
<i>Ascending Pass Images</i>					
26–27 Dec. 1995	E1-23262/E2-3589	1613 ^b	99	–33	used with Dec. 1995
30–31 Jan. 1996	E1-23763-E2-4090	1613 ^b	132		descending images to derive flow direction
8–9 Oct. 1997	E1-32595/E2-12922	1608 ^b	–94	↑	Oct. 1997

^aTopography baseline is the equivalent perpendicular baseline for the topography component of the differential combination of interferograms.

^bIndicates (and arrows) for a particular interferogram which other pair was used to remove the topographic signal.

^cLarger errors are expected in the velocity for May 1996, when the interferograms used in differential processing were formed from images from different satellite tracks.

sheets A5, B5, and B6). We also employed this DEM to determine ground control points beyond the margins of Monacobreen and for baseline refinement. Six interferometric DEMs for Monacobreen were produced (Table 1), with an estimated vertical accuracy of only 20 to 40 m due to the rugged topography and relatively low resolution of the map-derived DEM used for ground control.

[9] In order to remove the topographic phase signal and produce velocity-only interferograms we used the interferometrically derived DEM closest in time to each interferogram (Table 1). To help unwrap fringes, we used the displacement maps from one date as a model of velocity from other dates. Most velocity interferograms could be phase unwrapped from a known zero reference (a nunatak in the upper part of Monacobreen) to ~ 7 km from glacier front. In all eleven velocity maps were produced (Table 1).

3.2. Dual-Azimuth Processing

[10] In order to determine the full 3-D surface flow direction, data from three look directions are required [Joughin *et al.*, 1998; Mohr *et al.*, 1998]. ERS SAR provides two look directions from the ascending and descending passes of the satellite, and data from these can be combined using dual-azimuth processing to produce 2-D velocity fields. In the absence of in situ measurements, the vertical component of flow can be estimated from a DEM by assuming flow occurs parallel to the ice surface [e.g., Reeh *et al.*, 1999]. This assumption gives us the third dimension of the velocity field: the potential error associated with this assumption is discussed below.

[11] Data suitable for dual azimuth processing were only available in winter 1995/1996 (Table 1). In order to compute surface displacement maps for the other dates we

assumed the ice flow direction did not change during the surge. In order to verify this assumption, we used coherence tracking (explained below) [e.g., Rott *et al.*, 1998; Strozzi *et al.*, 2002] between descending image pairs to estimate the 2-D horizontal component of the flow direction. This analysis showed no significant change in flow direction during the surge, albeit at a reduced resolution. Furthermore, two dual-azimuth snapshots during the surge of Fridtjovbreen, Svalbard produced using the same techniques show a mean absolute change in flow direction of only 1.2° over 23 months despite an increase in velocity by 4 to 5 times [Murray *et al.*, 2003].

3.3. Intensity and Coherence Tracking

[12] Surge velocities close to the front of Monacobreen exceed those for which interferometric phase can be usefully interpreted. Therefore we applied a technique based on tracking the optimum correlation between image patches [Rott *et al.*, 1998; Michel and Rignot, 1999; Murray *et al.*, 2002; Strozzi *et al.*, 2002]. This technique can be applied successfully only where displacements between images are larger than ~ 1 m and derives displacement information at a much coarser resolution than interferometry. The procedure can use either the optimization of intensity correlation or the optimization of phase coherence within image patches.

[13] Intensity correlation tracking was used to derive surface velocities from Monacobreen near its front where displacement rates and chaotic surface change limited interferometric coherence. Coherence tracking was used in unwrapping the January and March 1994 data to tie a disconnected island of coherence to a velocity reference. Assuming an estimation error of 0.05 pixel in range and azimuth, the displacement error from the tracking techni-

ques is less than 1.2 m d^{-1} for tandem data and less than 0.4 m d^{-1} for SAR data with a 3-day repeat cycle [Strozzi *et al.*, 2002].

3.4. Potential Sources of Error

[14] There are no in situ field measurements of velocity that can be used as ground truth for our SRI velocity measurements. Joughin *et al.* [1998] and Fatland and Lingle [1994] provide discussion of the sources of error in 3-D estimation of velocity using SRI. These sources include systematic errors arising from changes in atmospheric water content, errors in the estimates of the baseline (the perpendicular distance between satellite positions at the time of acquisition), unwrapping errors, and errors in the DEM, as well as those arising from failure of the assumptions used in processing [Goldstein, 1995; Rignot *et al.*, 1996; Joughin *et al.*, 1999]. Changes in atmospheric water content are expected to be small during high latitude winter, so that the resulting uncertainty in phase is expected to be at most ± 0.25 cycle [Gray *et al.*, 1997]. This phase change is equivalent to ± 0.005 and $\pm 0.02 \text{ m d}^{-1}$ in the ground range direction for 3-day and tandem data respectively. In this study, baselines were calculated from precision orbit models except for the ERS-1 1997 ascending data when ERS-1 precision orbits were not available. Uncertainty from this source is expected to be less than $\pm 0.01 \text{ m d}^{-1}$. Unwrapping faults will lead to integer multiples of 2π errors in unwrapped phase. These will lead to errors in velocity in multiples of ± 0.02 and $\pm 0.07 \text{ m d}^{-1}$ for 3-day and tandem data, respectively, in the ground range direction. The magnitude of the systematic errors in the flow rate can be assessed by the maximum apparent surface displacement of rock areas other than those used as a zero velocity reference. After masking areas of ice and water using data from digital maps (NP 1:100,000 map sheets A5, B5, and B6), mean displacement values were $\sim 0.1 \text{ m d}^{-1}$ for the 1997 ascending mode data when precision orbits were not available, and $\sim 0.05 \text{ m d}^{-1}$ for all other dates.

[15] The processing sequence we have used relies on three assumptions:

[16] 1. Differential processing assumes that both the surface topography and the displacement rate remain constant between the images used. A change in topography between interferograms will lead to a corresponding velocity error. For a perpendicular baseline of 50 m, a relatively large change in topography of 50 m between interferograms will lead to an error of only 0.007 m d^{-1} [Joughin *et al.*, 1996b], which can be considered to be negligible in this study. If the velocity has changed between the pairs of scenes used to form differential interferograms, this will result in errors in the separation of topography and velocity. As long as the velocity varies systematically, the resulting error in velocity cannot be greater than the change in velocity [Luckman *et al.*, 2002]. In general, the resulting error will be smaller for triplets of images separated by 3 days and larger for tandem data.

[17] 2. The assumption of surface parallel flow has been commonly used to derive the vertical component of flow for valley and outlet glaciers [e.g., Rignot *et al.*, 1996; Vachon *et al.*, 1996; Mohr *et al.*, 1998; Rott *et al.*, 1998; Mattar *et al.*, 1998; Joughin *et al.*, 1999]. However, this assumption has limitations because flow is in general submergent in the

accumulation zone and emergent in the ablation zone [Reeh *et al.*, 1999]. In steady state, these vertical components are equal to the local mass balance. Surge-type glaciers exist in a state perpetually out of balance with the local climate. The vertical component of flow can be accounted for if the ice thickness is known [Reeh *et al.*, 1999], which unfortunately is not the case for Monacobreen. On the quiescent-phase surge-type Black Rapids Glacier, Alaska, the surface parallel assumption was shown to result in errors of up to $\sim 20\%$ or $\sim 0.03 \text{ m d}^{-1}$ in the magnitude of 3-D velocity [Rabus and Fatland, 2000]. These errors could be largely removed by using a seasonally adjusted vertical velocity of 0.002 to 0.003 m d^{-1} representing mass gain in the reservoir zone. Our study is undertaken in the active phase when vertical velocities could both be higher and have greater temporal variation.

[18] In order to make some estimate of the likely error resulting from the assumption of surface parallel flow, we use vertical velocity measurements made during the active phase of Bakaninbreen, Svalbard. Over the entire surge duration of between 5 and 10 years at Bakaninbreen, ice thinning in the reservoir zone was $\sim 15 \text{ m}$ and thickening in the receiving zone was 20 to 60 m [Murray *et al.*, 1998], so the rate of thickening or thinning varied from -0.008 to $+0.03 \text{ m d}^{-1}$. The ERS SAR configuration is much more sensitive to vertical than horizontal displacements because of the steep look angle. If we assume that the glacier surface is flat, a vertical displacement d_v would be misinterpreted as a horizontal displacement of d_h

$$d_h = \frac{d_v}{\tan \theta_d \cos(\varphi_f - \varphi_d)}, \quad (1)$$

where φ_d and φ_f are the orientation angle of the SAR observation, and ice flow directions respectively, and θ_d is the incidence angle of the SAR observation. Vertical velocity equivalent to values from Bakaninbreen would result in a horizontal velocity error of up to $\sim \pm 0.07 \text{ m d}^{-1}$ if the flow direction coincides with the satellite look direction. The error will increase as the angle between the incidence angle and flow direction increases. For an angle between the flow direction and look direction of 30° , the error is $\sim \pm 0.08 \text{ m d}^{-1}$, and as this angle increases to 75° the error increases to about $\sim \pm 0.27 \text{ m d}^{-1}$.

[19] 3. As discussed earlier, because of the scarcity of ascending scenes in the data archive, we assumed that the flow direction did not vary during the surge. The magnitude r of the three-dimensional displacement vector can be computed by

$$r = \frac{r_d}{\sin \theta_d \cos \nu_f \cos(\varphi_f - \varphi_d) + \cos \theta_d \sin \nu_f}, \quad (2)$$

where r_d is the magnitude of the displacement in the look direction of the SAR. In order to make an estimate of error, we again assume the glacier is flat, i.e., ν_f is zero. By representing with φ the difference ($\varphi_f - \varphi_d$) between flow and look directions we obtain

$$r = \frac{r_d}{\sin \theta_d \cos \varphi}. \quad (3)$$

The error with respect to the difference between the flow and look direction is therefore

$$\partial r = \frac{r_d}{\sin \theta_d} \frac{\sin \varphi}{\cos^2 \varphi} \partial \varphi, \quad (4)$$

and the relative error is

$$\frac{\partial r}{r} = \tan(\varphi) \partial \varphi. \quad (5)$$

Using equation (5), an estimate of the effect of a change in the ice flow direction during the surge can be made. For a 5° change in flow direction, the error is $\sim 5\%$ when the angle between the flow direction and look direction is 30° . As this angle increases to 75° , the error increases to about 30%.

[20] Because the error in the calculated velocity increases rapidly with increasing angle between ice flow direction and look direction (discussion points 2 and 3 above), all data within $\pm 15^\circ$ of perpendicular to the look direction were masked from the 3-D velocity maps when only descending data were available.

4. Results

[21] The 34 ERS SAR scenes used in this study (Table 1) allowed the computation of 18 interferograms (e.g., Figure 2). The fringe visibility on these interferograms is strongly related to the ice surface displacement field. For example, a strip of ice from a tributary glacier on the eastern side of Monacobreen was coherent right to the glacier front in the early surge interferograms (arrow on Figure 2a), becoming activated by the surge between March 1992 and January 1994 (Figures 2b and 2c). Clearly visible on the interferograms are shear margins at each side of the glacier with spatially high rates of change of displacement manifested as a high fringe rate (Figures 2a–2c). In October 1997, the glacier was coherent over virtually its whole surface suggesting that the flow rate had dropped dramatically (Figure 2d).

[22] As discussed above, the direction of ice flow at all times was assumed to be the same as the flow field for winter 1995–1996, which was the only time for which dual-azimuth data were available (Table 1 and Figure 3). Figure 4 shows eleven temporal snapshots of 3-D surface velocity on Monacobreen between 1991 and 1997 superimposed on the SAR intensity images, which have been calibrated to be directly intercomparable in brightness. Any residual brightness differences in these images will result from differing local conditions between the acquisitions chosen (e.g., changes in snow water content or surface roughness). The greatly increased brightness, particularly in 1994 (Figure 4), almost certainly reflects increased surface roughness due to intense crevassing at this time. Glacier velocity increased progressively from 1991 to 1994 and then decreased, showing an apparent temporary increase over the whole glacier between December 1995 and May 1996 (Figure 4). It should be noted that greater errors are expected in the May measurement because the interferograms used in differential processing were formed from images from different satellite tracks (Table 1). Surface velocity measurements are available only where coherence levels permitted

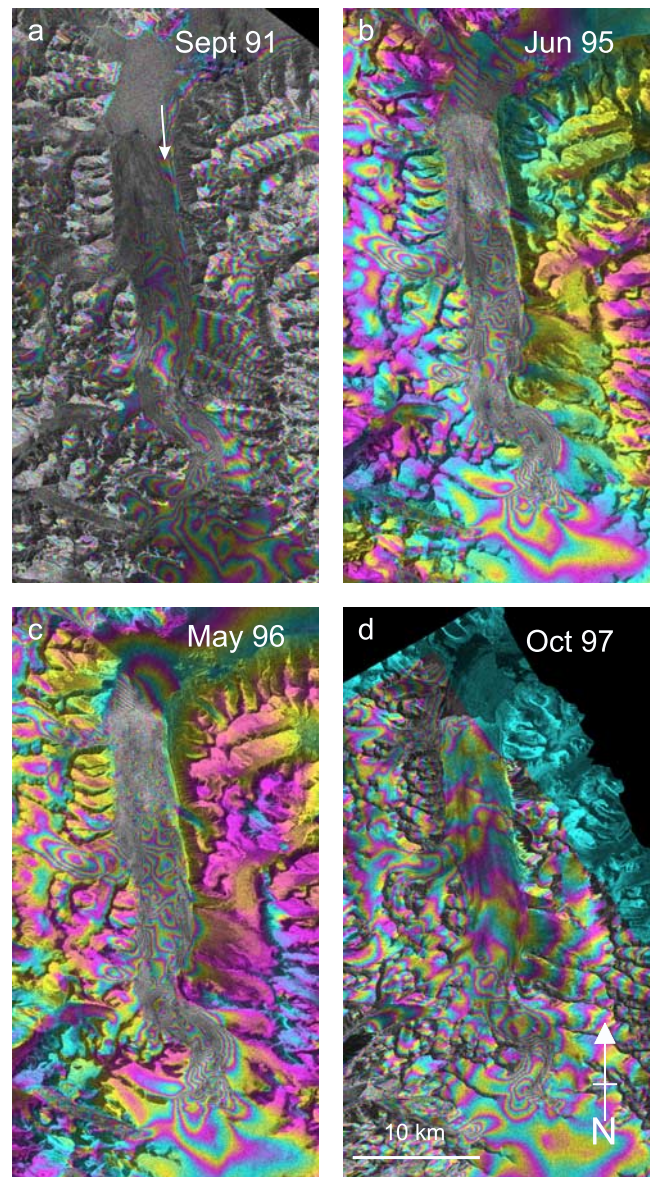


Figure 2. Selected geocoded interferograms over Monacobreen. Baselines are given in Table 1. These interferograms contain information on both topography and displacement in the look direction of the sensor. Hue indicates interferometric phase with color intensity modulated by the SAR backscatter. Interferograms formed from scenes in June 1995 and May 1996 have a very short topographic baseline and are therefore virtually insensitive to topography. In northern Svalbard, the look direction is (a–c) 126° for descending data and (d) 238° for ascending data at an incidence angle of 23° to the vertical.

phase unwrapping (Figure 4). Velocity values are more extensive during and after 1995 when tandem (1-day repeat) data were available (Table 1), and the glacier was beginning to slow down. This increase in coverage results because the interferometric phase coherence is increased by decreases in either velocity or repeat-pass delay.

[23] The spatial differences in the velocity fields are most easily compared using profiles oriented upglacier (Figure 5) and cross-glacier (Figure 6). The main velocity increase

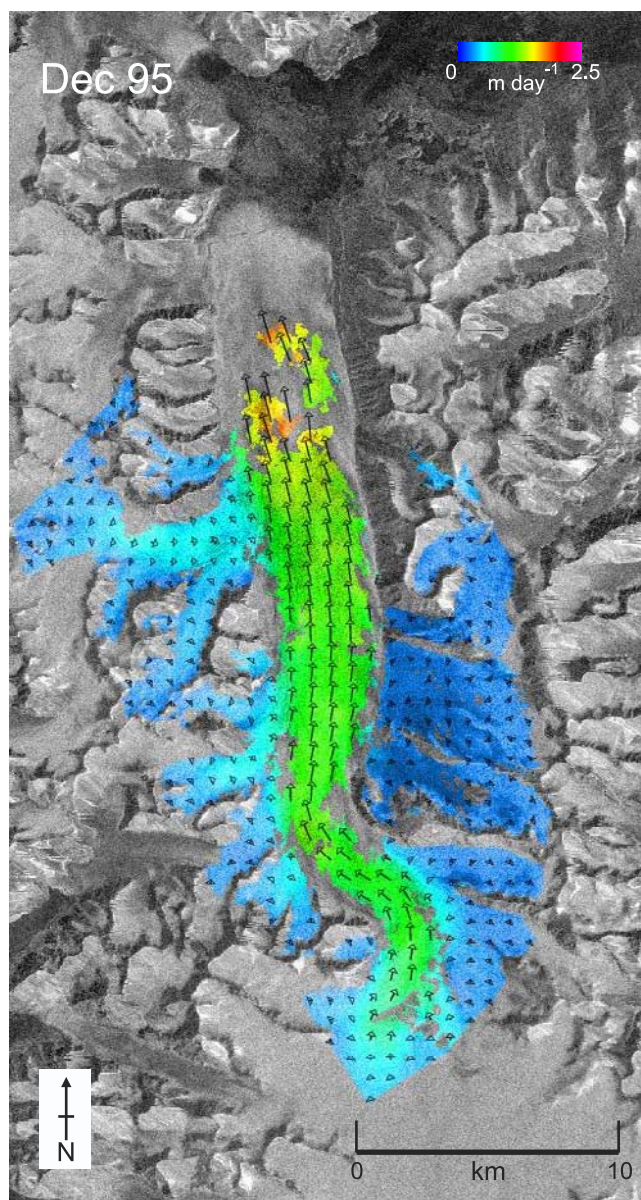


Figure 3. The 3-D velocity derived from winter 1995–1996 dual-azimuth differential interferometry shown as color (hue) modulated by SAR backscatter (intensity). Ice flow direction for all other times was taken from these results. Velocity arrows are displayed every 750 m. Surface velocity measurements are available only where coherence levels permitted phase unwrapping. Background image is SAR backscatter.

occurred uniformly, initially in the lower part of the glacier, with the velocity more than doubling between September 1991 and March 1992 (Figure 5a). This initial increase in velocity predominantly affected the bend in the glacier and areas downglacier of km 22. (This notation refers to the location on the flow line shown in Figure 1 with km 0 being the December 1995 margin; for example, km 22 refers to a location 22 km upglacier of km 0). The velocity in the upper part of the glacier did not increase substantially until January 1994 (Figure 5a). There was no indication of a

surge front or activation wave travelling downglacier, and if this occurred, it did so before September 1991. The cross profiles (Figure 6) showed generally flat cross sections. Only X6, located farthest upglacier, showed a parabolic cross section. Finally, while the velocity increased dramatically during the surge, the pattern of velocity, especially the locations of local maxima and minima, remained remarkably consistent throughout the surge.

[24] We could not use interferometry to map the velocity over the entire glacier surface because coherence was lost close to the sides and at the front. The problem was most acute when the velocity was greatest (Figures 2 and 4). Intensity correlation tracking shows that the velocity increased very rapidly toward the glacier front (approximately downglacier of km 8.5) to velocities over $\sim 5 \text{ m d}^{-1}$ (Figure 7).

[25] The longitudinal velocity profiles allow calculation of strain rates (Figure 8). During the surge, strain rates on Monacobreen increased to $\sim 0.001 \text{ d}^{-1}$ (0.37 yr^{-1}), which is greater than the rates of $< 0.1 \text{ yr}^{-1}$ typical of most non-surge glaciers [Kamb *et al.*, 1985]. While strain rates increased as the velocity increased, in general, many locations on the flow line that were locally extensile or compressive remained consistent in space (Figure 8).

[26] From these results, we can also investigate the temporal evolution of the glacier surge. Figure 9a shows how the velocity at three locations on the glacier surface (A, B, and C in Figure 1) changed during the six years of observation. These three sample points were chosen as they have valid measurements from every differential observation and as they are representative of the whole glacier. The velocity increased steadily between September 1991 and March 1992 with a remarkably constant rate of change during this period. We have therefore fit straight lines to the data by least squares regression, and for these lines the coefficients of determination (R^2) vary between 0.97 and 1.00. Between January 1994 and October 1997, the velocity dropped, again approximately linearly, and although the R^2 values are lower, they are still remarkably high (0.93 to 0.97). The gradient of these lines gives the acceleration or deceleration of the glacier at each location. This graph shows that the switch between surge acceleration and deceleration occurred during the period when there are no data available (after the second ice phase of ERS-1 and before the tandem mission), and strongly suggests that maximum flow rates occurred during 1993.

[27] This temporal analysis is extended to every point on the flow line in Figure 9b, which shows the acceleration, deceleration and associated coefficients of determination. During surge acceleration (September 1991 to March 1992), the coefficient of determination was close to 1.0 downglacier from $\sim \text{km } 28$ suggesting that the velocity was increasing systematically. Upglacier from km 28, the linearity of the relationship breaks down. The rate of acceleration increases from $\sim \text{km } 28$ to $\sim \text{km } 18$, downglacier from which point the pattern of acceleration peaks and troughs corresponds to the pattern of velocity peaks and troughs: regions of higher velocity experience greater velocity increases than regions of lower velocity. During surge deceleration (January 1994 to October 1997), the coefficient of determination was lower but was still greater than ~ 0.8 downglacier of km 27. In general, the deceleration rate

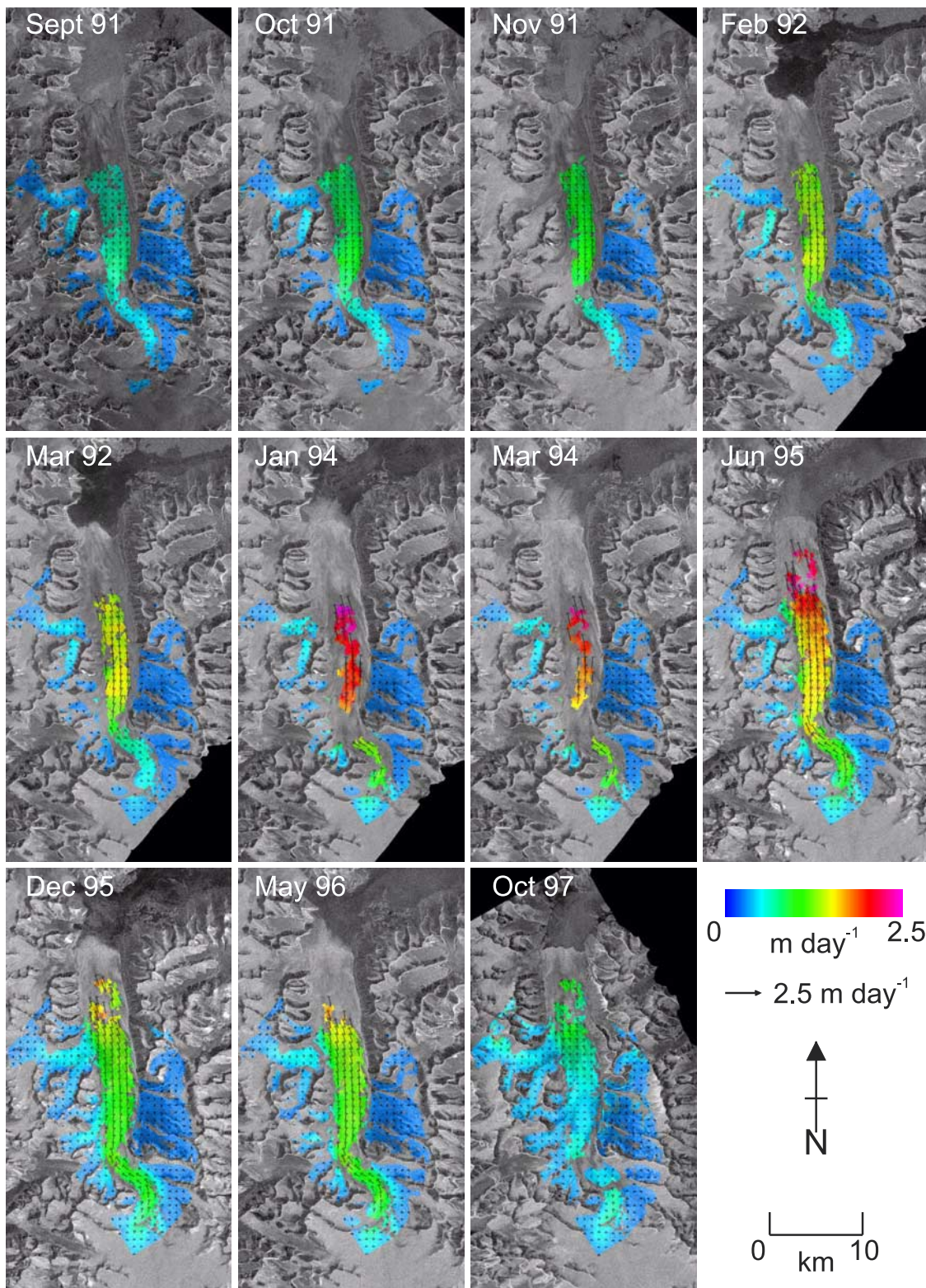


Figure 4. Plan view velocity maps from September 1991 to October 1997 showing 24 x 45 km area of Monacobreen and its surroundings. Where surface displacement rates have been retrieved, hue indicates velocity (see color scale) with color intensity modulated by the SAR backscatter. Background image is SAR backscatter, calibrated so that intensity is directly comparable throughout the sequence.

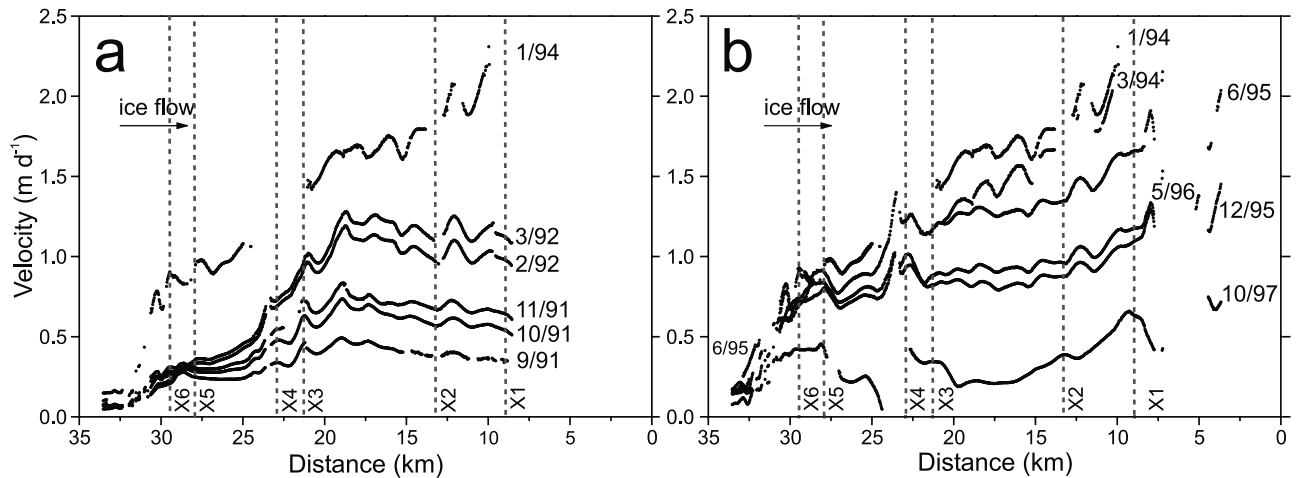


Figure 5. Time series of velocity from interferometry along long profile of Monacobreen (location in Figure 1). (a) Progressive velocity increase from September 1991 to January 1994 and (b) progressive velocity decrease from January 1994 to October 1997, with a temporary possible velocity increase between December 1995 and May 1996. Gaps in the data indicate regions that were incoherent and could not be unwrapped in the interferometric image at the location of the transect or where the flow direction approached an angle perpendicular to the line of sight. X1–X6 indicate the locations of the cross profiles presented in Figure 6.

increases steadily downglacier and the deceleration rate was approximately one third the acceleration rate.

[28] SAR intensity images at approximately annual intervals were used to track the terminus position (Figure 10). The glacier advanced ~ 2 km after September 1991 and was at maximum extent in April 1996. Between April 1996 and October 1997 the central section retreated more than 250 m, while the western and eastern sections still advanced ~ 100 m. Between October 1997 and September 1998 the entire front margin was in retreat. The maximum measured advance rate of the glacier terminus was during winter 1991–1992, and this preceded the velocity peak in January 1994 (Figures 5 and 10). Terminus retreat started once the ice flow velocity fell to ~ 2 m d $^{-1}$ close to the glacier front.

5. Discussion

5.1. Velocity During Quiescence

[29] An approximation of the velocity during the quiescent phase on Monacobreen can be made by assuming glacier flow is due solely to ice creep. In this case, the ice creep velocity u_q may be approximated by

$$u_q = \tau_d^n H^2 A / (n + 1), \quad (6)$$

where τ_d is the basal shear stress, $n = 3$ and $A = 2.4 \times 10^{-15}$ s $^{-1}$ kPa $^{-3}$ at -2° C are flow law parameters, and H is the ice thickness [Paterson, 1994, p. 251]. If we assume the basal shear stress is equal to the gravitational driving stress then

$$\tau_d = F \rho_i g H \sin \alpha, \quad (7)$$

where F is a valley shape factor, ρ_i is the density of ice, g is the gravitational constant, and α is the ice surface slope. We do not have any ice thickness measurements for Monacobreen as the RES study failed to penetrate to the glacier bed [Bamber, 1987]. An estimate, however, can be made using

an empirical relationship between glacier thickness and surface area, S ,

$$H = 33 \ln S + 25, \quad (8)$$

which is valid for Svalbard outlet glaciers with surface areas greater than 1 km 2 [Hagen *et al.*, 1993]. Monacobreen has a surface area of ~ 408 km 2 [Hagen *et al.*, 1993] and hence a predicted thickness of ~ 225 m. The shape factor, F , is therefore ~ 1 [Paterson, 1994, p. 269]. The average surface slope is $\sim 2^\circ$, so the gravitational driving stress is ~ 69 kPa (equation (7)) and, using equation 6 with the full range of ice densities quoted by Paterson [1994, p. 9], the creep velocity is ~ 2.2 to 3.0 m yr $^{-1}$ (0.006 to 0.008 m d $^{-1}$).

[30] These values are significantly less than the lowest velocity we measured on Monacobreen. However, they are comparable to those measured on Svalbard surge-type glaciers during quiescence such as Bakaninbreen (~ 0.2 to 0.4 m yr $^{-1}$) [Murray *et al.*, 1998], Finsterwalderbreen (~ 1 to 5 m yr $^{-1}$) [Nuttall *et al.*, 1997], Kongsvegen (~ 2.9 m yr $^{-1}$) [Melvold and Hagen, 1998], and Sefstrømbreen (~ 2 m yr $^{-1}$) [Liestøl *et al.*, 1980]. The calculation suggests that the increase in velocity between the quiescent and active phase at Monacobreen is ~ 100 to 1000 times. The very large contrast in velocity between the calculated creep velocity and our measured velocities suggest that basal motion (sliding or sediment deformation) dominates flow during the active phase of glacier surging.

5.2. Characteristics of the Surge of Monacobreen

5.2.1. Acceleration and Deceleration Phases

[31] Figure 9a shows two phases during Monacobreen's surge: namely a months-long acceleration phase (September 1991 to March 1992), and longer and more progressive deceleration phase. We do not have data from this study to observe transitions between either of these states and quiescence, nor between acceleration and deceleration.

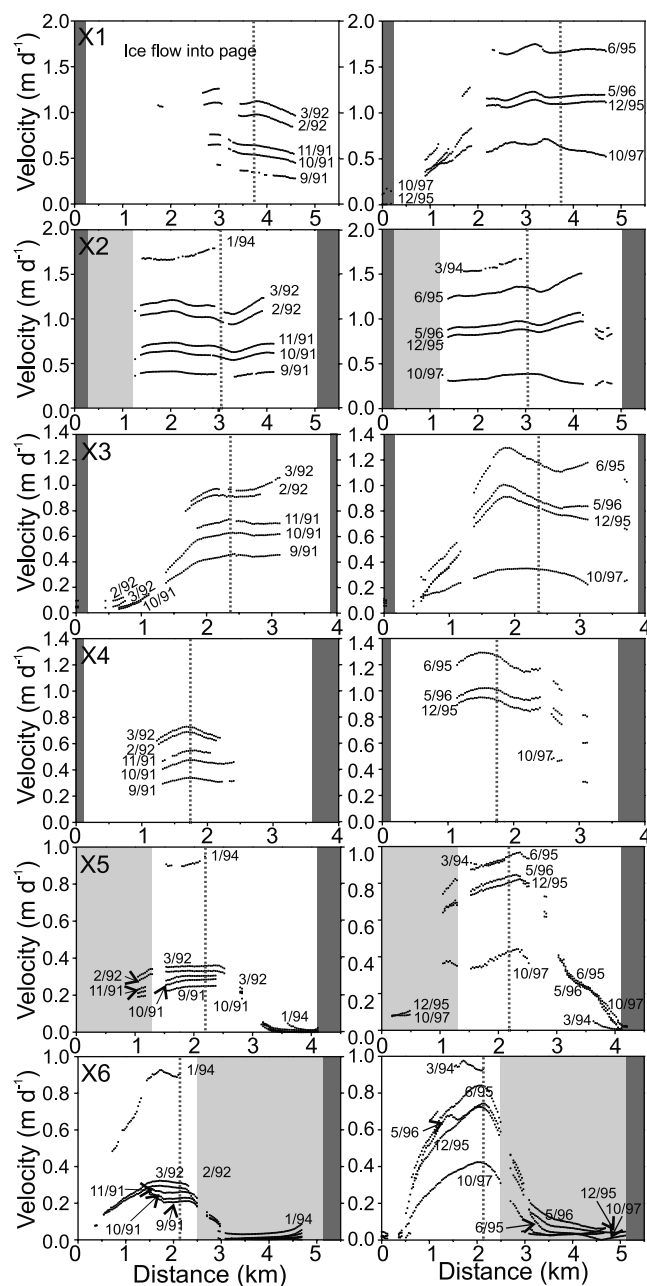


Figure 6. Time series of cross glacier velocity profiles (locations in Figure 1). (left) Increasing velocities (September 1991 to January 94) and (right) the decreasing velocities (March 1994 to October 1997). Transects were chosen approximately perpendicular to the flow line and extend, where possible, from valley side to valley side. Dark gray zones indicate rock, and light gray zones indicate a different flow unit or tributary. Gaps in the data indicate regions that were incoherent and could not be unwrapped in the interferometric image or where the flow direction approached an angle perpendicular to the line of sight. The dotted line indicates the intersection with the long profile.

[32] Our observations span only those months with low surface temperatures because of the need to maintain coherence. This sampling strategy means that any velocity variations that occur during the summer months may not

be observed. However, the increase of velocity between September 1991 and March 1992 is monotonic (Figure 9). The decrease between January 1994 and October 1997 is broken only by a temporary apparent increase in flow rate between December 1995 and May 1996. Prior to the May 1996 images, surface temperatures had been below zero (mean -5.4°C) for the previous 19 days (data collected in Ny Ålesund by Norske Meteorologiske Institutt), so this variation is unlikely to have been driven by surface melt. We believe that short-lived or seasonal velocity variations are subdued compared to the overall velocity cycle of acceleration and deceleration we have revealed.

5.2.2. Spatial Pattern of Velocity During Active Phase

[33] We have no evidence of a surge front propagating downglacier on Monacobreen. Such a surge front would be expected to be marked by closely spaced fringes in interferograms or by incoherence because of the high spatial rate of change in velocity. A surge front could have reached the glacier front before our observations began, but this seems unlikely given the relatively low ice velocities measured. Rather, the surge appeared to start simultaneously over the entire lower region of the glacier and then to propagate upglacier. Two other studies of Svalbard surges also report no surge front. At both Osbornebreen [Rolstad *et al.*, 1997] and Fridtjovbreen [Murray *et al.*, 2003] the surge is reported to have started at the glacier terminus and to have propagated upglacier. In contrast, Bakaninbreen had a clear surge front [Murray *et al.*, 1998], and at Usherbreen crevassing started in the upper part of the glacier and propagated downglacier [Hagen, 1987]. We note that those glaciers where a surge front has been reported are land terminating, whereas glaciers without reported surge fronts terminate in water deep enough to calve at their termini (Table 2).

5.2.3. Static Nature of Velocity Pattern in Space

[34] Surge velocities on Monacobreen were as much as 5.0 m d^{-1} (Figures 4–6), and in general increased downglacier, especially close to the glacier margin (Figures 5 and 7). On other Svalbard glaciers reported surge velocity magnitudes are similar (Table 2). We noted earlier that the local pattern of both velocity and strain rate at Monacobreen are remarkably consistent throughout the surge (Figures 5 and 8), so that whatever controls the spatial distribution of velocity must remain fixed throughout the surge phase. Furthermore, as the flow rate increases the difference between velocity highs and lows also increases. In other words, those regions that are “sticky spots” at low velocity became relatively stickier, and the “slippery spots” became more slippery as the velocity increased. The spatial pattern of surge velocity has been observed for only a very few glaciers in Svalbard. At Osbornebreen, tracking of crevasses on Landsat and SPOT imagery during 1988 showed generally extensile flow with velocities varying between 0.0 to 6.0 m d^{-1} [Rolstad *et al.*, 1997].

[35] Controls on glacier flow fall into two groups, those which would be expected to change during a surge (e.g., thermal structure, basal sediment composition, the effect of tributary glaciers, structure of the basal water system and input of surface water), and those that would remain constant (e.g., bedrock features and valley shape). The wavelength of spatial variation in velocity and strain rate is much less than variations in overall valley shape (compare Figures 1, 5, and 8). Furthermore, the variations in

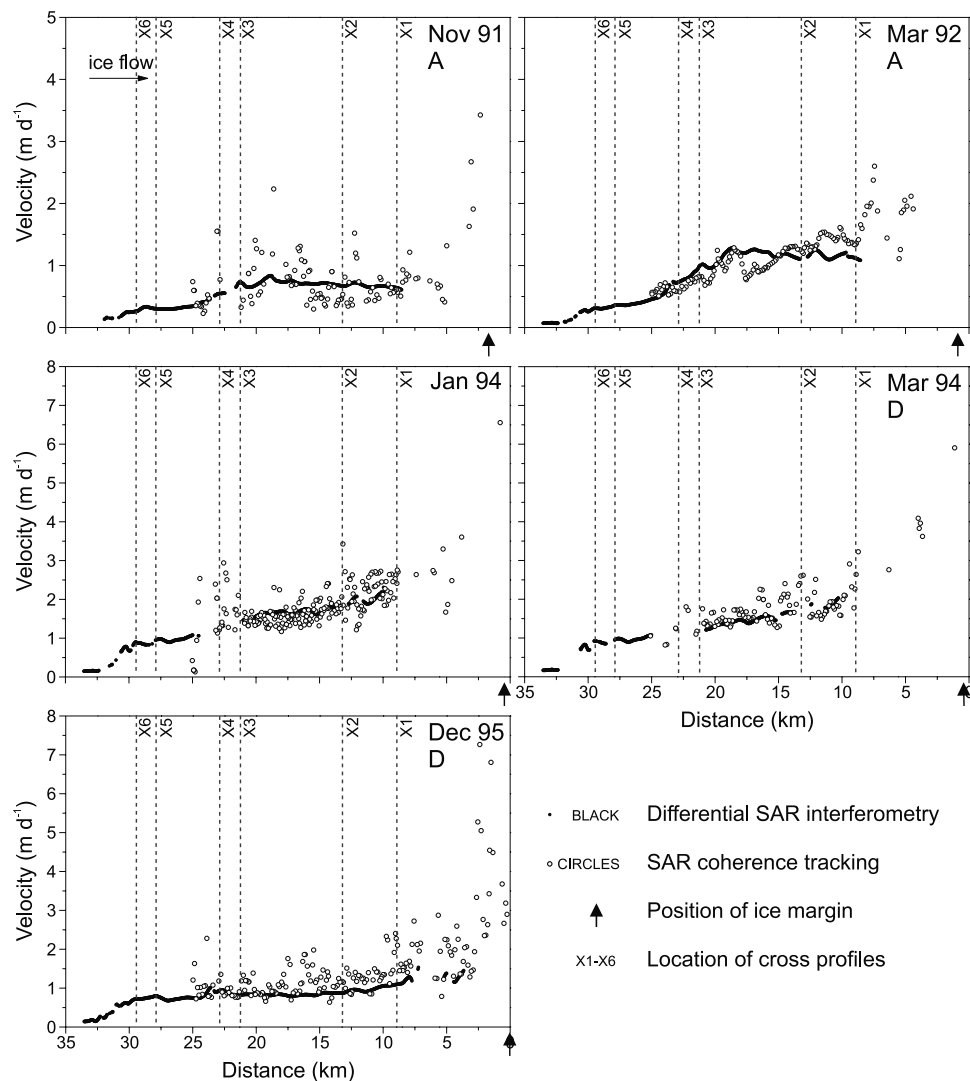


Figure 7. Time series of velocity from differential SAR interferometry (solid line) and intensity correlation tracking (open circles). A, acceleration phase; D, deceleration phase. January 1994 is the fastest measured flow rate. Intensity correlation tracking data are displayed from km 25 to the ice margin (variable over the years) and give velocity data where SRI measurements are missing due to regions of poor coherence or where the flow direction approached an angle perpendicular to the line of sight.

velocity and strain rate appear to be regularly spaced, whereas variations in valley shape are irregularly spaced. We therefore believe that the main controls on the small-scale glacier velocity are basal bedrock features.

5.2.4. Surge Duration

[36] We do not believe that we captured the full surge with these SRI observations. This assertion is based on the following: (1) there is no change of shape in the velocity cross profiles with time, and hence no change in the dominant flow mechanism over our observation period; (2) there is no evidence of a switch on or off in either the flow rate or the acceleration or deceleration; (3) the estimated quiescent-phase velocity is much lower than our observed velocities; and (4) the glacier was already advancing at the start of our observations. We therefore believe that the active phase was longer than the 73 months (more than six years) of our observations. Extrapolation of the linear trends in Figure 9a to the calculated

quiescent velocities suggests that the surge started between early January and late May 1991 and ended between November 1998 and January 2002. In early May 1991, there were no significant crevasses on Monacobreen, which suggests that strain rates were quite low at this time, whereas the following year it was heavily crevassed (J. O. Hagen, personal communication, 2001). Therefore our estimate of the active phase duration is 89 to 133 months (7 to 11 years), which is in keeping with observations of active phases (3–10 years) on other Svalbard glaciers [Dowdeswell *et al.*, 1991].

5.3. A Typical Svalbard Surge Cycle

[37] In Figure 11a we have used the results from this study, and results from the literature to reconstruct glacier dynamics during a “typical Svalbard glacier surge cycle.” Overall cycle lengths in the archipelago are thought to be 50–500 years [Dowdeswell *et al.*, 1991] but are not well

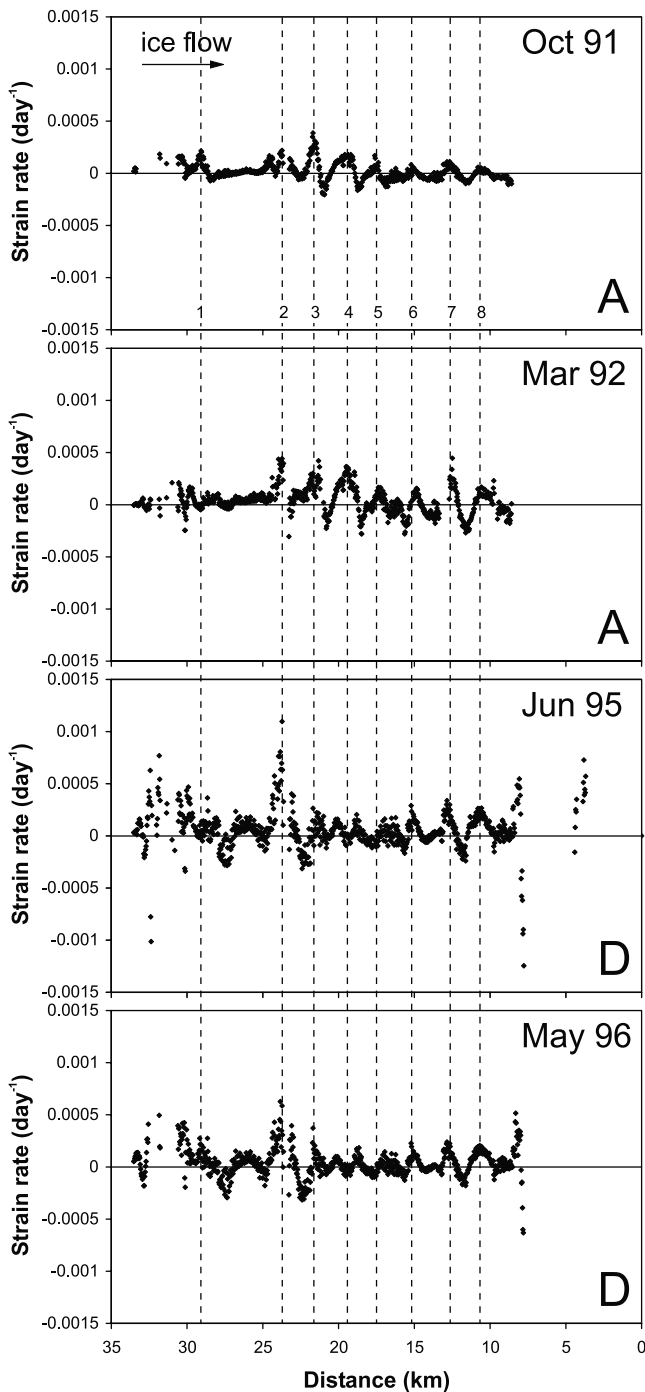


Figure 8. Profiles of longitudinal strain rate along long profile of Monacobreen for surge acceleration (A) and deceleration (D). Profile location is shown in Figure 1. The dashed and numbered lines 1 to 8 show the location of prominent compressional strain rate anomalies in early surge. Most anomalies remain throughout the surge, although amplitudes change, e.g., 2, 3, 6, 7, 8; others switch from compressional to extensile, e.g., 4, 5; others switch off and reoccur later, e.g., 1.

known as only five glaciers have been observed to surge twice. Observed surge intervals have been between 40 (Tunabreen) and 133 years (Fridtjovbreen) [Hagen *et al.*, 1993]. It is likely that the duration of the average surge

cycle in Svalbard is longer than these intervals. The surge starts with a years-long period of steady acceleration, which was measured at Fridtjovbreen using similar methods to this study [Murray *et al.*, 2003]. This is followed by a months-long period of relatively rapid acceleration that we see at both Monacobreen (Figure 9) and Fridtjovbreen [Murray *et al.*, 2003]. The length of the active phase is typically 3–10 years [Dowdeswell *et al.*, 1991], and was probably between 7 and 11 years at Monacobreen. The end of the fast flow phase is very gradual, with velocity decreasing over a years-long period (Figure 9). The characteristic of a much longer and more progressive termination on Svalbard glaciers is confirmed by data from Kongsvegen, where flow rates ~ 20 years after the surge started were still $\sim 1 \text{ m d}^{-1}$, whereas after 45 years they were $\sim 0.008 \text{ m d}^{-1}$ [Melvold and Hagen, 1998].

5.4. Contrasts With Surges of Glaciers in Other Regions, Especially Those of Variegated Glacier

[38] The best studied glacier surge is probably the 1982–1983 surge of Variegated Glacier in Alaska [e.g., Kamb *et al.*, 1985] (Table 2), and the dynamics of this surge are

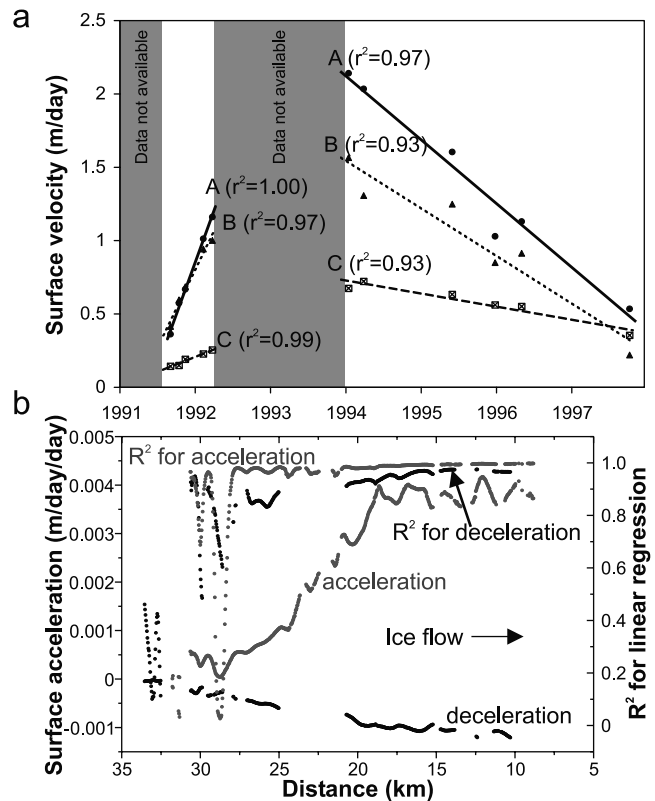


Figure 9. (a) Surface velocity as a function of time for positions A, B, and C on the glacier (Figure 1). Gray areas indicate times when data suitable for SRI were not available. Straight-line fits show the linearity of the rate of change of velocity for both the acceleration and the deceleration phases of the surge. (b) Rate of change of velocity with respect to time and associated coefficient of determination (R^2) for the entire flow line shown in Figure 1. Gray indicates surge acceleration (September 1991 to March 1992). Black indicates surge deceleration (January 1994 to October 1997). See text for full explanation.

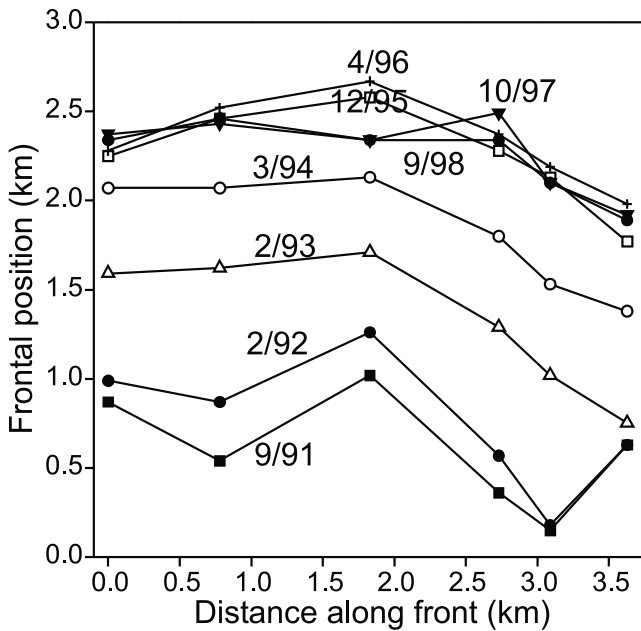


Figure 10. Position of the glacier terminus between September 1991 and September 1998 obtained from tracking six points along a 3.5 km west to east transect. Displacements are estimated to be accurate to ± 1 pixel or about ± 30 m.

summarized in Figure 11b. Its surge was characterized by extreme basal water pressures and a highly tortuous, high volume basal water system that had low water throughflow rates, postulated to be a linked cavity system [Kamb *et al.*, 1985; Kamb, 1987]. The surge occurred in two phases, the first beginning in the winter of 1982 in the upper part of Variegated Glacier, which accelerated to a maximum in late June 1982 before slowing abruptly over a few hours. The velocity then decreased until August/September, although there were major pulses of increased motion superimposed on this decelerating trend. The second phase began in the upper part of the glacier in October 1982 and propagated progressively downglacier activating the lower region of the glacier. Surge velocities were ~ 10 to 50 $m\ d^{-1}$ and strain rates at the surge front were $\sim 0.2\ d^{-1}$. Evidence for the nature of the basal water system during the surge came from dye tracing [Kamb *et al.*, 1985]. During the surge, dye transit velocities were slow ($0.025\ m\ s^{-1}$) and the dye appeared at the margin at a number of outlet streams. After the surge, the dye appeared rapidly (transported at a velocity of $\sim 0.7\ m\ s^{-1}$) at a single outlet stream.

[39] The surge terminated extremely rapidly over a few hours on 4 July 1983, and by September the whole glacier was moving at less than presurge velocities. The termination was marked by an outburst flood of turbid water, an abrupt drop in the pressure in the basal water system, and a drop in the glacier surface of ~ 0.1 m. This very rapid termination is inferred to have resulted from the collapse of basal cavities and formation of an efficient tunnel based drainage system. Similarly rapid surge terminations (\sim days) were seen at Medvezhiy Glacier, Pamirs [Osipova and Tsvetkov, 1991] and West Fork Glacier, Alaska [Harrison

Table 2. Comparison of the Surge of Monacobreen With Other Surges^a

Glacier	Length, km	Area, km ²	Surge Date	Surge Duration, years	Quiescence Duration, years	Surge Advance, km	Drawdown, m	Thickening, m	Basal Shear Stress, kPa	Quiescent Velocity, $m\ d^{-1}$	Typical Surge Velocity, $m\ d^{-1}$	Surge Front Propagation, $m\ d^{-1}$	Source
Variegated	20	29	five times in 20th century	2	16–26	2–5	50	110	160–180	0.1–1.0	~ 50	23–80	1
Finsterwalder	11	45	1900s			1.5	50	100	40–95	0.002–0.03		no front	2
Fridtjov ^b	13	49	1860s, 1990s	4+	130	>2.5			105	0.08–0.3	2.0–3.3	possible front	3, 4
Usher	13	69	1980s	7		1.5	40	>100	33–61		1.5–4.3		5, 6
Bodley ^b	16	87	1970–1980s	4–13		2.7	10–15	10–60		0.05–0.5	2.0–2.6		5, 7
Bakanin	17	61	1980–1990s	5–10	>85	0	15+	20–60	52–66	0.001	1–3	0.9–4.5	8
Osborne ^b	20	152	1980s	4+		2	100	100			1.2–6.0	no front	5, 9
Seifström ^b	23	155	1880s			6.5				0.005	1.3		10
Kongsvegen	26	102	before 1948			1.5–2.0				0.008	>1.0		11
Tuna ^b	35	203	1930, 1970		50	1.5							12
Monaco ^b	42	408	1990s	6+		2				0.005–0.008	0.5–5.0	no front	
Himlopen ^b	68	1250	1970s	4+		3					14–16		6

^aAll glaciers except Variegated Glacier are located in Svalbard.

^bGlaciers terminate in water sufficiently deep to calve at their terminus.

Data sources: 1, Kamb *et al.* [1985], Raymond *et al.* [1987], and Wilbur [1988]; 2, Nuttall *et al.* [1997]; 3, A.-M. Nuttall (personal communication, 2000); 4, Murray *et al.* [2002b]; 5, Dowdeswell *et al.* [1991]; 6, Hagen [1987]; 7, Dowdeswell and Collin [1990]; 8, Murray *et al.* [1998]; 9, Rolstad *et al.* [1997]; 10, Boulton *et al.* [1997]; 11, Melvold and Hagen [1998]; 12, Hodgkins and Dowdeswell [1994].

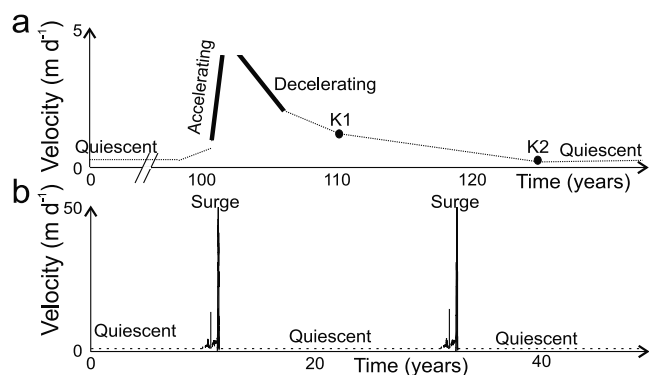


Figure 11. (a) Schematic summary of the dynamics of glacier surging on Monacobreen and other Svalbard glaciers. Bold lines are the data from this study, the dotted line showing the early slow (years-long) part of the acceleration phase is taken from a related study of Fridtjovbreen [Murray *et al.*, 2003], and K1 and K2 are velocity measurements ~ 20 years and ~ 45 years after the start of the surge of Kongsvegen [Melvold and Hagen, 1998]. (b) Variegated Glacier, a surge thought to be promoted by linked cavity formation and terminated by their collapse (data from Kamb *et al.* [1985]). Quiescence is characterized by seasonal cycles in velocity with faster flow in summer than winter [Raymond and Harrison, 1988] and minisurges [Kamb and Engelhardt, 1987], neither of which are shown on this figure. The initiation of the surge of Variegated Glacier was less abrupt than the termination, whereas the opposite is true on Monacobreen.

et al., 1994]: all are in stark contrast to the prolonged terminations of surging observed in Svalbard. At West Fork Glacier, termination was associated with floods of turbid water. Large outburst floods also marked the termination of fast flow of Bering Glacier, Alaska [Molnia, 1994], and water pressures during the surge were extremely high, as evidenced by the presence of pressurized basally derived water in crevasses [Herzfeld and Mayer, 1997]. Turbid water was also seen in supraglacial lakes and marginal crevasses during the surge of Peters Glacier, Alaska [Echelmeyer *et al.*, 1987]. The surge of Sortebræ, east Greenland, was characterized by very high ice velocities, extreme basal water pressures, and a rapid termination [Murray *et al.*, 2002]. All these surges had ice dynamics similar to those of Variegated Glacier.

[40] Figure 11 summarizes the major contrasts in dynamics between the surges of Svalbard glaciers and those of Variegated Glacier. Flow velocities on Variegated Glacier were an order of magnitude higher and strain rates two orders of magnitude higher than those measured on Monacobreen. On Variegated Glacier, there would appear to be two states: surging, when the glacier is underlain by a linked cavity hydraulic system, and quiescent, when the glacier is underlain by a channelled water system. These states are in contrast to the three states inferred for Monacobreen. Variegated Glacier switches rapidly between these two states, although the switch from slow to fast flow (weeks to months) is less rapid than the switch from fast to slow flow (two days) (Figure 11a). In contrast, on Monacobreen acceleration was more rapid than deceleration. During the

surge of Variegated, the flow rate was highly variable, whereas on Monacobreen we have no evidence for significant short-lived velocity variations.

5.5. Evidence Against the Linked Cavity Mechanism of Surging Operating in Svalbard

[41] The linked cavity mechanism provides a good model for surging at many Alaskan glaciers. We do not believe however that the linked cavity mechanism is applicable to the surge of Monacobreen or other Svalbard glaciers suggests that the termination mechanism in the archipelago is fundamentally different from that of Variegated Glacier.

[42] 1. On Variegated Glacier, the glacier stopped almost instantaneously, coinciding with the release of a large amount of turbid and therefore probably basal water. Kamb [1987] explained the termination of glacier surging of Variegated as resulting from the collapse of a linked cavity water system into a channelled water system. The very slow surge termination on Monacobreen and other Svalbard glaciers suggests that the termination mechanism in the archipelago is fundamentally different from that of Variegated Glacier.

[43] 2. There are no reports of basal water in marginal lakes or water-filled crevasses during surges of Svalbard glaciers. Such lakes or water-filled crevasses are used to support assertions of basal water systems that are large volume and high water pressure (i.e., have characteristics similar to linked cavity systems) beneath surging glaciers in other regions [Lingle *et al.*, 1994; Reeh *et al.*, 1994; Jiskoot *et al.*, 2001].

[44] 3. There is no evidence of short-lived, large-scale velocity variations during Svalbard surges. Such velocity variations appear to be characteristic of the surge of Variegated Glacier. Any such velocity variations are subdued on Svalbard glaciers.

[45] 4. The linked cavity theory predicts that glaciers with low slope are more likely to be of surge-type [Kamb, 1987; Clarke, 1991]. Statistical studies have shown that in Svalbard, surge-type glaciers tend to be steeper than normal glaciers [Jiskoot *et al.*, 1998].

[46] Given the strong evidence for the linked cavity mechanism of surging for Variegated Glacier and that against its operation in Svalbard, we suggest that there exist at least two different surge mechanisms.

5.6. Possible Surge Mechanism in Svalbard

[47] Our observations of Monacobreen allow inferences to be made about basal conditions during the surge event. The glacier is polythermal and was most likely warm based over the majority of its length during our observations. The glacier is probably soft bedded, but bedrock features control its large-scale velocity pattern. These basal conditions are probably common beneath Svalbard surge-type glaciers. Statistical studies have shown that such glaciers tend to be polythermal and to overlie sedimentary bedrock [Hamilton and Dowdeswell, 1996; Jiskoot *et al.*, 1998, 2000]. The results of these studies, together with field observations of polythermal regimes [Murray *et al.*, 2000; Smith *et al.*, 2002] and deforming sedimentary beds [e.g., Porter and Murray, 2001] beneath Svalbard surge-type glaciers, are thought to support a thermally regulated soft bed surge mechanism in Svalbard. Similar basal conditions also occur beneath Trapridge Glacier, Yukon Territory [e.g.,

Clarke *et al.*, 1984; Clarke and Blake, 1991]; however, no observations have yet been made at this glacier in its active phase.

[48] Fowler *et al.* [2001] present a model of thermally regulated surging over a soft bed that we believe may be applicable to our observations at Monacobreen as well as other Svalbard glaciers: (1) At the start of the surge cycle (quiescence) the glacier is cold based or polythermal. In the former case, ice builds up until the pressure melting point is reached over some portion of the glacier bed. (2) Once the pressure melting point is reached, basal meltwater is produced and leads to elevated pore water pressures and weakening of the underlying till. (3) These increased pore water pressures cause deformation and hence dilation of the till, increasing water storage and further weakening it. (4) Accelerated deformation of the basal till produces frictional heating, which results in further melting and raises pore water pressures at the glacier bed. (5) The positive feedback between basal motion and meltwater production continues resulting in rapid basal motion. (6) This basal motion continues causing ice thinning until increased heat loss results in refreezing at the glacier bed.

[49] The critical model parameters are the thickness and permeability of unfrozen till [Fowler *et al.*, 2001], which together govern the efficiency of meltwater evacuation from the bed, and thus control basal water pressure. If the thickness and permeability are both low, basal drainage is impeded, effective pressure can reach zero and surging can occur. If the till thickness and permeability are close to, but above threshold values, dynamic oscillations can occur, but without a very rapid flow phase. The rate of surge onset is primarily controlled by the thickness of unfrozen till, because this controls the volume of meltwater required to reach overburden pressure, while the rate of ice flow during a surge is controlled by the bed roughness or by friction at the glacier sides.

[50] Once the basal water pressure rises and the effective pressure reaches zero, the water is conceived of as being stored in “blisters” formed at the ice-bed interface [Fowler *et al.*, 2001]. If basal water pressure is high enough to cause decoupling of the glacier from its bed or the opening of faults through the ice, discharge of water from these blisters will occur. The blisters are not supposed to play a significant role in promoting glacier flow, although discharge from them is significant during surge termination. At a certain ice thickness, blister discharge becomes sufficiently high to reestablish normal effective pressures. In general, the rate of surge termination is controlled by ice thinning, which in turn is controlled by the rate of transport of ice downglacier (i.e., slow surges should have slow terminations).

[51] In this model, the fronts between surging and non-surging ice are seen as propagating both up and downglacier as a “thermal activation wave”, i.e., the transition between cold and warm ice [cf. Murray *et al.*, 2000]. Two types of surge are suggested by the Fowler *et al.* [2001] model. In the first, the propagation of the activation wave is slow relative to the ice speed, and this causes a wall of ice to propagate downglacier (as at Bakaninbreen and Usherbreen). In other words, the thermal activation front is also the surge front. If the propagation of the activation wave is faster than ice flow, the surge is gentler. Lack of a surge front (as observed at Monacobreen) can result if there is no

restriction to flow at the margin. This can occur if the glacier base is at the melting point all the way to the terminus, and is even more likely if the glacier terminates in tidewater sufficiently deep to calve [c.f., Hodgkins and Dowdeswell, 1994]. Hence the model may be able to explain the differences observed between tidewater and land terminating surging glaciers in Svalbard.

[52] We believe that our observations started somewhere between steps 2 and 4 of the cycle described above and continue into step 6 but not into full quiescence. Notable aspects of the model with respect to our observations are that (1) the rate of flow during the surge is controlled by the form drag at the bed (this is in keeping with our inference that sticky spots at Monacobreen result from bedrock obstructions and that these become increasingly important as the flow rate increases) and (2) the model can explain the lack of an observed surge front, the progressive surge initiation, prolonged active phase duration and slow termination.

6. Conclusions

[53] Using a combination of differential interferometry and intensity correlation tracking we have elucidated, in unprecedented detail, the spatial and temporal development of glacier dynamics during a surge of Monacobreen. We infer a three-phase surge cycle: acceleration, deceleration and quiescence. The 6-year SRI sequence of velocity measurements covers part of the acceleration and deceleration phases. Surge acceleration was approximately three times more rapid than deceleration. Surge dynamics at Monacobreen are in marked contrast to the observed surge of Variegated Glacier in Alaska [Kamb *et al.*, 1985], which started relatively progressively and terminated over a period of only a few hours. The contrast in dynamics of Monacobreen and other Svalbard glaciers with Variegated Glacier make it very unlikely that the same surge mechanisms are involved. We therefore hypothesize that there exist at least two markedly different types of glacier surges.

[54] **Acknowledgments.** ESA provided the ERS images under project AO3-283. Meteorological data were kindly supplied by the Norske Meteorologiske Institutt and digital map data by NP. This project is funded by the UK Natural Environment Research Council (GST/02/2192 and F14/6/37). We thank U. Wegmüller and D. Vaughan for their contributions to the analysis and discussion, B. Kulesa and A. Fowler for comments on the text, and J.O. Hagen for drawing our attention to the surge of Monacobreen. The referees (R. LeB. Hooke and J.O. Hagen) and associate editor (T. Pfeffer) have worked hard to improve this paper, for which we thank them.

References

- Bamber, J. L., Radio echo sounding of Svalbard glaciers, Ph.D. thesis, 207 pp., Scott Polar Res., Inst., Univ. of Cambridge, Cambridge, U.K., 1987.
- Boulton, G. S., J. J. M. van der Meer, J. Hart, D. Beets, G. H. J. Ruegg, F. M. van der Wateren, and J. Jarvis, Till and moraine emplacement in a deforming bed surge—An example from a marine environment, *Quat. Sci. Rev.*, 15, 961–987, 1996.
- Clarke, G. K. C., Length, width and slope influences on glacier surging, *J. Glaciol.*, 37(126), 236–246, 1991.
- Clarke, G. K. C., and E. W. Blake, Geometric and thermal evolution of a surge-type glacier in its quiescent state: Trapridge Glacier, *Yukon Territory, Canada, 1969–89*, *J. Glaciol.*, 37(125), 158–169, 1991.
- Clarke, G. K. C., S. G. Collins, and D. E. Thompson, Flow, thermal structure and subglacial conditions of a surge-type glacier, *Can. J. Earth Sci.*, 21(2), 232–240, 1984.
- Dowdeswell, J. A., and R. L. Collin, Fast-flowing outlet glaciers on Svalbard ice caps, *Geology*, 18, 778–781, 1990.

- Dowdeswell, J. A., G. S. Hamilton, and J. O. Hagen, The duration of the active phase on surge-type glaciers: contrasts between Svalbard and other regions, *J. Glaciol.*, 37(127), 388–400, 1991.
- Dowdeswell, J. A., B. Unwin, A.-M. Nuttall, and D. J. Wingham, Velocity structure, flow instability and mass flux on a large Arctic ice cap from satellite radar interferometry, *Earth Planetary Sci. Lett.*, 167, 133–140, 1999.
- Echelmeyer, K., R. Butterfield, and D. Cuillard, Some observations on a recent surge of Peters Glacier, *Alaska, J. Glaciol.*, 33(115), 341–345, 1987.
- Fatland, D. R., and C. S. Lingle, Analysis of the 1993–95 Bering Glacier (Alaska) surge using differential SAR interferometry, *J. Glaciol.*, 44(148), 532–546, 1998.
- Fowler, A. C., T. Murray, and F. S. L. Ng, Thermal regulation of glacier surging, *J. Glaciol.*, 47(159), 527–538, 2001.
- Goldstein, R., Atmospheric limitations to repeat-track radar interferometry, *Geophys. Res. Lett.*, 22(18), 2517–2520, 1995.
- Gray, A. L., K. E. Mattar, D. Geudtner and P. W. Vachon, Experiments at CCRS using ERS tandem mode data, in *3rd ERS Scientific Symposium, 17–21 March 1997, Florence, Italy Proceedings*, vol. 2, *Eur. Space Agency Spec. Publ., ESA SP-414*, 1001–1006, 1997.
- Hagen, J. O., Glacier surge at Usherbreen, *Svalbard, Polar Res.*, 5, 239–252, 1987.
- Hagen, J. O., O. Liestøl, E. Roland, and T. Jørgensen, Glacier atlas of Svalbard and Jan Mayen. *Medd. 129*, 140 pp., Nor. Polarinst., Tromsø, Norway, 1993.
- Hamilton, G. S., and J. A. Dowdeswell, Controls on glacier surging in Svalbard, *J. Glaciol.*, 22(140), 157–168, 1996.
- Harrison, W. D., K. A. Echelmeyer, E. F. Chacho, C. F. Raymond, and R. J. Benedict, The 1987–88 surge of West Fork Glacier, Susitna Basin, Alaska, U.S.A., *J. Glaciol.*, 40(135), 241–254, 1994.
- Herzfeld, U. C., and H. Mayer, Surge of Bering Glacier and Bagley Ice Field, Alaska: An update to August 1995 and an interpretation of brittle-deformation patterns, *J. Glaciol.*, 43(145), 427–434, 1997.
- Hjelle, A., and Ø. Lauritzen, Geological map of Svalbard 1: 500 000, sheet 3G Spitsbergen northern part, *Nor. Polarinst. Skr.*, 154C, 1982.
- Hodgkins, R., and J. A. Dowdeswell, Tectonic processes in Svalbard tidewater glacier surges: Evidence from structural glaciology, *J. Glaciol.*, 40(136), 553–560, 1994.
- Jiskoot, H., P. J. Boyle, and T. Murray, The incidence of glacier surging in Svalbard: Evidence from multivariate statistics, *Comput. Geosci.*, 24(4), 387–399, 1998.
- Jiskoot, H., T. Murray, and P. J. Boyle, Controls on the distribution of surge-type glaciers in Svalbard, *J. Glaciol.*, 46(154), 412–422, 2000.
- Jiskoot, H., A. K. Pedersen, and T. Murray, Multi-model photogrammetric analysis of the 1990s surge of Sortebrae, *East Greenland, J. Glaciol.*, 47(159), 677–687, 2001.
- Joughin, I., D. Winebrenner, M. Fahnestock, R. Kwok, and W. Krabill, Measurement of ice-sheet topography using satellite radar interferometry, *J. Glaciol.*, 42(140), 10–22, 1996a.
- Joughin, I., R. Kwok, and M. Fahnestock, Estimation of ice-sheet motion using satellite radar interferometry: Method and error analysis with application to Humboldt Glacier, Greenland, *J. Glaciol.*, 42(142), 564–575, 1996b.
- Joughin, I., R. Kwok, and M. Fahnestock, Interferometric estimation of three-dimensional ice-flow using ascending and descending passes, *IEEE Trans. Geosci. Remote Sens.*, 36(1), 25–37, 1998.
- Joughin, I., M. Fahnestock, R. Kwok, P. Gogineni, and C. Allen, Ice flow of Humboldt, Petermann and Ryder Gletscher, northern Greenland, *J. Glaciol.*, 45(150), 231–241, 1999.
- Kamb, B., Glacier surge mechanism based on linked cavity configuration of the basal conduit system, *J. Geophys. Res.*, 92, 9083–9100, 1987.
- Kamb, B., and H. Engelhardt, Waves of accelerated motion in a glacier approaching surge: The mini-surges of Variegated Glacier, Alaska, U.S.A., *J. Glaciol.*, 33(113), 27–46, 1987.
- Kamb, B., et al., Glacier surge mechanism: 1982–1983 surge of Variegated Glacier, *Alaska, Science*, 227(4686), 469–479, 1985.
- Kwok, R., and M. A. Fahnestock, Ice sheet motion and topography from radar interferometry, *IEEE Trans. Geosci. Remote Sens.*, 34(1), 189–200, 1996.
- Liestøl, O., K. Repp, and B. Wold, Supraglacial lakes in Spitsbergen, *Nor. Geogr. Tidsskr.*, 34, 89–92, 1980.
- Lingle, C. S., A. Post, U. C. Herzfeld, B. F. Molnia, R. M. Krimmel, and J. J. Roush, Correspondence: Bering Glacier surge and iceberg-calving mechanism at Vitus Lake, Alaska, U.S.A., *J. Glaciol.*, 39(133), 722–727, 1994.
- Luckman, A., T. Murray, and T. Strozzi, Satellite flow evolution throughout a glacier surge measured by satellite radar interferometry, *Geophys. Res. Lett.*, 29(23), 2095, doi:10.1029/2001GL014570, 2002.
- Mattar, K. E., P. W. Vachon, D. Geudtner, A. L. Gray, I. G. Cumming, and M. Brugman, Validation of Alpine glacier velocity measurements using ERS tandem-mission SAR data, *IEEE Trans. Geosci. Remote Sens.*, 36(3), 974–984, 1998.
- Melvold, K., and J. O. Hagen, Evolution of a surge-type glacier in quiescent phase: Kongsvegen, Spitsbergen, 1964–95, *J. Glaciol.*, 44(147), 394–404, 1998.
- Michel, R., and E. Rignot, Flow of Glacier Moreno, Argentina, from repeat-pass shuttle imaging radar images: Comparison of the phase correlation method with radar interferometry, *J. Glaciol.*, 45(149), 93–100, 1999.
- Mohr, J. J., N. Reeh, and S. N. Madsen, Three-dimensional glacial flow and surface elevation measured with radar interferometry, *Nature*, 391, 273–276, 1998.
- Molnia, B. F., The 1993–1994 surge of Bering Glacier, Alaska, slide captions, pp. 1–4, U.S. Geol. Surv., Reston, Va., 1994.
- Murray, T., J. A. Dowdeswell, D. J. Drewry, and I. Frearson, Geometric evolution and ice dynamics during a surge of Bakaninbreen, *Svalbard, J. Glaciol.*, 44(147), 263–272, 1998.
- Murray, T., G. W. Stuart, P. J. Miller, J. Woodward, A. M. Smith, P. R. Porter, and H. Jiskoot, Glacier surge propagation by thermal evolution at the bed, *J. Geophys. Res.*, 105, 13,491–13,507, 2000.
- Murray, T., T. Strozzi, A. J. Luckman, H. D. Pritchard, and H. Jiskoot, Ice dynamics during a surge of Sortebrae, East Greenland, *Ann. Glaciol.*, 34, 323–329, 2002.
- Murray, T., A. J. Luckman, T. Strozzi, and A.-M. Nuttall, The initiation of glacier surging at Fridtjovbreen Svalbard, *Ann. Glaciol.*, 36, in press, 2003.
- Nuttall, A.-M., J. O. Hagen, and J. A. Dowdeswell, Quiescent-phase changes in velocity and geometry of Finsterwalderbreen, a surge-type glacier in Svalbard, *Ann. Glaciol.*, 24, 249–254, 1997.
- Osipova, G. B., and D. G. Tsvetkov, Kinematics of the surface of a surging glacier (comparison of the Medvezhiy and Variegated Glaciers), *IAHS Publ.*, 208, 345–357, 1991.
- Paterson, W. S. B., *The Physics of Glaciers*, 3rd ed., 480 pp., Pergamon, New York, 1994.
- Porter, P. R., and T. Murray, Hydrological and mechanical properties of till beneath Bakaninbreen, Svalbard, *J. Glaciol.*, 47(157), 167–175, 2001.
- Rabus, B. T., and D. R. Fatland, Comparison of SAR-interferometric and surveyed velocities on a mountain glacier: Black Rapids Glacier, Alaska, U.S.A., *J. Glaciol.*, 46(152), 119–128, 2000.
- Raymond, C. F., and W. D. Harrison, Evolution of Variegated Glacier, Alaska, U.S.A., prior to its surge, *J. Glaciol.*, 34(117), 154–169, 1988.
- Raymond, C. F., T. Johannesson, T. Pfeffer, and M. Sharp, Propagation of a glacier surge into stagnant ice, *J. Geophys. Res.*, 92, 9037–9049, 1987.
- Reeh, N., C. E. Bøggild, and C. Oerter, Surge of Storstrømmen, a large outlet glacier from the inland ice of north-east Greenland, *Rapp. Grønlands Geol. Unders.*, 162, 201–209, 1994.
- Reeh, N., S. N. Madsen, and J. J. Mohr, Combining SAR interferometry and the equation of continuity to estimate the three-dimensional glacier surface-velocity vector, *J. Glaciol.*, 45(151), 533–538, 1999.
- Rignot, E., R. Forster, and B. Isacks, Interferometric radar observations of Glacier San Rafael, Chile, *J. Glaciol.*, 42(141), 279–291, 1996.
- Rolstad, C., J. Amlin, J. O. Hagen, and B. Lundén, Visible and near-infrared digital images for determination of ice velocities and surface elevation during a surge on Osbornbreen, a tidewater glacier in Svalbard, *Ann. Glaciol.*, 24, 255–261, 1997.
- Rott, E., M. Stuefer, A. Siegel, P. Skvarca, and A. Eckstaller, Mass fluxes and dynamics of Moreno Glacier, Southern Patagonia Icefield, *Geophys. Res. Lett.*, 25(9), 1407–1410, 1998.
- Smith, A. M., T. Murray, B. Davison, A. F. Clough, J. Woodward, and H. Jiskoot, Late-surge glacial conditions on Bakaninbreen, Svalbard and implications for surge termination, *J. Geophys. Res.*, 107(B8), 10.1029/2001JB000475, 2002.
- Strozzi, T., A. Luckman, T. Murray, U. Wegmüller, and C. Werner, Glacier motion using satellite-radar offset tracking procedures, *IEEE Trans. Geosci. Remote Sens.*, 40(11), 2384–2391, 2002.
- Vachon, P. W., D. Geudtner, K. E. Mattar, M. Brugman, and I. Cumming, Differential SAR interferometry measurements of Athabasca and Saskatchewan glacier flow rate, *Can. J. Remote Sens.*, 22(3), 287–296, 1996.
- Wilbur, S. C., Surging versus nonsurging glaciers: A comparison using morphometry and balance, MSc. thesis, 113 pp., Univ. of Alaska, Fairbanks, 1988.
- P. Christakos and T. Murray, School of Geography, University of Leeds, Leeds LS2 9JT, UK. (panos@freeuk.com; tavi@geog.leeds.ac.uk)
- H. Jiskoot, Department of Geography, University of Lethbridge, 4401 Univ. Drive, Calgary, Alberta, Canada T1K 3M4. (hester.jiskoot@uleth.ca)
- A. Luckman, Department of Geography, University of Wales, Swansea, SA2 8PP, UK. (A.Luckman@swansea.ac.uk)
- T. Strozzi, Gamma Remote Sensing, Thunstrasse 130, CH-3074 Muri BE, Switzerland. (strozzi@gamma-rs.ch)